Transactions on the Built Environment vol 19, © 1996 WIT Press, www.witpress.com, ISSN 1743-3509

Vibration of rotating Timoshenko beams with centrifugal stiffening and specified torque or velocity profiles

D.C.D. Oguamanam,[a] G.R. Heppler[b]
[a]*Institute for Aerospace Studies, University of Toronto, 4925 Dufferin Street, Downsview, Ontario, Canada M3H 5T6*
[b]*ConStruct Group, Systems Design Engineering, University of Waterloo, Waterloo, Ontario, Canada N2L 3G1*

Abstract

A flexible beam with a tip mass and attached to a rotating base is modelled to include the tensile forces due to centripetal acceleration. The equations of motion are derived using the extended Hamilton's Principle and an approximate solution is approached via the Rayleigh-Ritz method. The system is simulated for both a prescribed torque profile and a prescribed velocity profile. The results indicate that the beam stiffens when these tensile forces are included. This is evidenced by an increased frequency and reduced amplitude of the flexural vibration of the beam.

1 Introduction

The use of structures that can be modelled as a rotating beam is very common in spacecraft applications. Thus it is not surprising that there is a large amount of literature on the dynamics and vibration of such structures. While these structures have previously been designed with rather stiff materials, there is a growing trend to use more flexible, light-weight materials. This is of particular interest in space and robotics applications.

Analytical expressions for the frequency equations and mode shapes of a Timoshenko beam for six common boundary configurations have been presented by Haung [1]. Huang's study was extended by White and Heppler [2] who provide generalized frequency equations and mode shapes that covered a wider range of boundary conditions than those presented by Huang. They observe that the contribution of the first moment of the mass of the tip mass is negligible when compared to the effect of the second moment of the tip mass.

Mitchell and Bruch [3] considered a model that is identical to [2] except that they use the Euler-Bernoulli beam theory and introduce a complaint hub. The Euler-Bernoulli theory was also used in the study by Bellezza *et al.* [4] who propose two formulations, pseudo-pinned and pseudo-clamped, which are derived from their choice of two non-inertial reference frames. A treatment of the Timoshenko beam which parallels the work of Bellezza *et al.* is given by White and Heppler [5].

The transverse vibration of a rotating flexible link for a prescribed velocity profile has been investigated by Kojima [6] for the case of an Euler-Bernoulli beam where an approximate formulation is obtained via the Galerkin method, and the transients are deduced by Laplace transformations.

The aforementioned studies all consider a rotating beam but neglect centripetal acceleration effects which are often referred to as the geometric stiffening effect. A probable reason for the exclusion of geometric stiffening in the above studies, as presented by Bellezza *et al.* [4], (for robotics applications) is that speeds capable of introducing substantial centrifugal forces into the system are rarely encountered in practice. However, it is clear that a rotating beam will experience axial forces due to centripetal acceleration. It would also seem reasonable to expect that the beam will experience an effective axial stiffening due to these inertial forces. What is not clear is just how fast does the beam have to be rotating for this effect to be meaningful and what is the magnitude of the stiffening effect with increasing angular velocity of the hub.

An attempt in this direction was made by Yigit *et al.* [7] who extended the work of Kojima [6] by including the centripetal acceleration contribution in their formulation. Yigit *et al.* [7] model the beam using Euler-Bernoulli

theory and derive an approximate solution using the Galerkin method. A simulation of the resulting equations of motion was done for the case with a prescribed torque profile. Although a tip mass was included while deriving the equations of motion, this was ignored in the simulation results that were presented. Nevertheless, they concluded that the linearized model—in which the elastic deformation is assumed not to affect the rigid-body motion—wrongly predicts the dynamics of the beam.

A similar conclusion was made by Damaren and Sharf [8] who investigated modelling flexible-link manipulators with various combinations of inertial and geometric nonlinearities. They concluded that the ability to correctly predict the dynamics of fast manœuvring manipulators decreases with increasing linearization. This conclusion was latter echoed by Sadigh and Misra [9]. The issue of geometric stiffening in multi-body dynamics has also been addressed[10].

The objective of this paper is to present the continuous and discrete formulations of the governing equations of motion of a rotating Timoshenko beam (including the centripetal acceleration contributions). We thereby hope to increase our understanding of the effect of centrifugal stiffening on the dynamics of a rotating flexible beam with a tip mass. We assume small deformations and choose the Timoshenko beam theory because it provides superior results when higher modes are necessary and when the beam is short [1, 11, 12]. The equations of motion are derived using the extended Hamilton's Principle and an approximate result is obtained via the Rayleigh-Ritz method. The system is simulated for both prescribed torque and prescribed velocity profiles.

2 Description of the System

The system of interest, depicted in Fig. 1, is a beam attached to a rotating hub at one end and has a mass m_t attached to the other end. The material and geometrical properties of the beam are: Young's modulus E, the shear modulus G, the shear correction factor $\kappa = 5/6$, the volume mass density, ρ, the beam length L, cross-sectional area A, and height h. The moment of inertia of the tip mass is denoted by I_{m_t} while C_{m_t} represents the first moment of the tip mass. The hub inertia is denoted by I_h.

Coordinates (X, Y, Z) refer to a fixed inertial frame $\mathcal{F}_I$ and coordinates

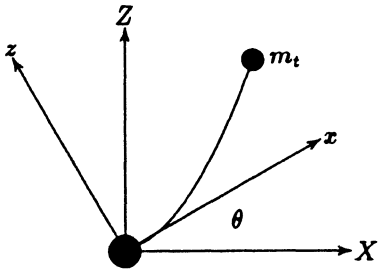

Figure 1: Schematic of the system.

(x, y, z) refer to the rotating frame $\mathcal{F}_r$; the basis vectors associated with $\mathcal{F}_I$ and $\mathcal{F}_r$ are chosen to be coincident at $t = 0$. The beam is assumed to rotate about the Y axis and it is further assumed that the elastic deflections are restricted to the XZ plane where only the transverse (i.e. in-plane) vibration is of interest. Axial deflection of the neutral axis (assumed to be coincident with the x axis) will be assumed to be negligible and, in keeping with assumptions of Timoshenko beam theory, plane sections are assumed to remain plane but not necessarily normal to the neutral axis after deformation.

3 Equations of Motion

Expressed in the rotating frame the assumed displacement field is

$$u(x, y, z, t) = \bar{u}(x, t) - z\psi(x, t) \quad (1)$$

$$v(x, y, z, t) = 0 \quad (2)$$

$$w(x, y, z, t) = \bar{w}(x, t) \quad (3)$$

where $\bar{u}(x, t)$ is the axial deflection of the reference (neutral) axis, $\bar{w}(x, t)$ is the transverse deflection of the reference (neutral) axis and $\psi(x, t)$ is the bending slope of the beam. The assumption that the beam does not undergo pure axial deformation requires $\bar{u}(x, t) = 0$.

The position vector of a general element of mass dm may be written as

$$\underset{\rightarrow}{r} = \underset{\rightarrow}{\mathcal{F}}_r^T \begin{bmatrix} x + u \\ 0 \\ z + w \end{bmatrix} = \underset{\rightarrow}{\mathcal{F}}_r^T \underset{\rightarrow}{r} \quad (4)$$

It is worth mentioning that $\underset{\rightarrow}{\mathcal{F}}_r$ and $\underset{\rightarrow}{\mathcal{F}}_I$ are vectrices (column matrices of basis vectors) [13].

The velocity of the elemental mass may be expressed as

$$\dot{\underset{\sim}{r}} = \underset{\sim}{r}^{\circ} + \underset{\sim}{\omega} \times \underset{\sim}{r} \tag{5}$$

where $(\,)^{\circ}$ indicates differentiation with respect to the rotating frame $\underset{\rightarrow}{\mathcal{F}}_r$. Thus, upon expansion, the velocity of the elemental mass is

$$\dot{\underset{\sim}{r}} = \underset{\rightarrow}{\mathcal{F}}_r^T \begin{bmatrix} -z\left(\dot{\psi}+\dot{\theta}\right) - \dot{\theta}\bar{w} \\ 0 \\ \dot{\bar{w}} + \dot{\theta}\left(x - \psi z\right) \end{bmatrix} \tag{6}$$

Using (6) the kinetic energy of the system, T, may be expressed as

$$T = \frac{1}{2}\Big\{\Big[I_h\left(\dot{\theta}+\dot{\psi}_0\right)\Big] + \Big[m_t\left(\dot{\bar{w}}_L^2 + \left(L^2+\bar{w}_L^2\right)\dot{\theta}^2 + 2\dot{\bar{w}}_L L\dot{\theta}\right) + I_{m_t}\left(\dot{\theta}^2\psi_L^2 + \left(\dot{\psi}_L+\dot{\theta}\right)^2\right) + C_{m_t}\left(\left(\dot{\psi}_L+\dot{\theta}\right)\dot{\theta}\bar{w}_L - \dot{\bar{w}}\psi_L\dot{\theta} - L\psi_L\dot{\theta}^2\right)\Big] + \left[\rho A\int_0^L\left(\dot{\bar{w}}^2 + \left(x^2+\bar{w}^2\right)\dot{\theta}^2 + 2\dot{\bar{w}}x\dot{\theta}\right)dx + \rho I\int_0^L\left(\dot{\theta}^2\psi^2 + \left(\dot{\psi}+\dot{\theta}\right)^2\right)dx\right]\Big\} \tag{7}$$

The first term (in [ ]) in the kinetic energy expression (7) is due to the rotational energy of the hub, the second term is from the motion of the mass at the tip of the beam, and the third term is the contribution of the beam.

The potential energy U of the system may be expressed as

$$U = \frac{1}{2}\int_0^L\left\{EI(\psi')^2 + \kappa GA(\bar{w}'-\psi)^2 + \left(m_t L + \frac{1}{2}\rho A\left(L^2-x^2\right)\right)\dot{\theta}^2(\bar{w}')^2\right\}dx \tag{8}$$

The first and second terms are the familiar bending and shear contributions, respectively, while the last term is the work done by the centrifugal forces due to the effects of the centripetal acceleration. To derive the contribution of the centrifugal forces, begin by defining the work done by the axial force W_{cp} as

$$W_{cp} \triangleq -\int_0^L F_{cp}(ds - dx) \tag{9}$$

where F_{cp} is the axial force, dx is the undeformed length of an infinitesimal element, and ds is the deformed length of the infinitesimal element. The deformed length is derived from $ds^2 = dx^2 + d\bar{w}^2$. By expressing ds in terms

of a binomial series, dropping the higher order terms, and re-arranging the resulting expression we can obtain

$$ds - dx = \frac{1}{2}(w')^2 dx \tag{10}$$

The total centrifugal force acting on the system due to centripetal acceleration can be expressed as

$$F_{cp} = m_t L\dot{\theta}^2 + \int_x^L \rho A x\dot{\theta}^2 dx = m_t L\dot{\theta}^2 + \frac{1}{2}\rho A\dot{\theta}^2\left(L^2 - x^2\right) \tag{11}$$

By using (10) and (11) in (9), we can find that

$$W_{cp} = -\int_0^L \left\{m_t L + \frac{1}{2}\rho A\left(L^2 - x^2\right)\right\}\frac{1}{2}\left(\dot{\theta}\bar{w}'\right)^2 dx \tag{12}$$

which corresponds to the last term in (8).

The virtual work done by the applied torque, $\delta\mathcal{W}_{tq}$, is given as

$$\delta\mathcal{W}_{tq} = \mathcal{M}\left(\delta\theta + \delta\psi_0\right) \tag{13}$$

A substitution of (7), (8), and (13) into the extended Hamilton's Principle results in nonlinear, coupled, integro-partial-differential equations of motion when variations are taken over $\bar{w}, \psi$, and θ [14]. The resulting equations are:

$$I_{tot}\ddot{\theta} + D_{tot}\dot{\theta} + \mu - \mathcal{M} = 0 \tag{14}$$

$$\rho A\left(x\ddot{\theta} + \ddot{\bar{w}} - \dot{\theta}^2\bar{w}\right) - \kappa GA\left(\bar{w}'' - \psi'\right) - \vartheta\dot{\theta}^2\bar{w}'' + \rho Ax\dot{\theta}^2\bar{w}' = 0 \tag{15}$$

$$\rho I\left(\ddot{\psi} + \ddot{\theta} - \dot{\theta}^2\psi\right) - \kappa GA\left(\bar{w}' - \psi\right) - EI\psi'' = 0 \tag{16}$$

The boundary conditions at $x = 0$ are: ,

$$\delta\bar{w}_0 = 0 \quad \text{and} \quad I_h\left(\ddot{\theta} + \ddot{\psi}_0\right) - EI\psi_0' - \mathcal{M} = 0 \tag{17}$$

The latter, in the case of a pseudo-pinned rotating frame model [5]. The boundary conditions at $x = L$ are:

$$\kappa GA\left(\bar{w}_L' - \psi_L\right) + m_t\left(\ddot{\bar{w}}_L - \bar{w}_L\dot{\theta}^2 + L\ddot{\theta} + L\dot{\theta}^2\bar{w}_L'\right) - C_{m_t}\left(2\dot{\psi}_L\dot{\theta} + \dot{\theta}^2 + \psi_L\ddot{\theta}\right) = 0 \tag{18}$$

$$EI\psi_L' + I_{m_t}\left(\ddot{\psi}_L + \ddot{\theta} - \dot{\theta}^2\psi_L\right) + C_{m_t}\left(L\dot{\theta}^2 + 2\dot{\bar{w}}_L\dot{\theta} + \ddot{\theta}\bar{w}_L\right) = 0 \tag{19}$$

The following definitions apply to the foregoing equations and boundary condition relations.

$$I_{tot} \triangleq I_{m_t} + I_h + \frac{\rho A L^3}{3} + \rho I L + m_t L^2 + m_t \bar{w}_L^2 + I_{m_t}\psi_L^2 + 2C_{m_t}(\bar{w}_L - L\Psi_L) + \int_0^L (\rho A \bar{w}^2 + \rho I \psi^2 - \vartheta(\bar{w}')^2) dx \quad (20)$$

$$D_{tot} \triangleq 2I_{m_t}\psi_L\dot{\psi}_L + 2m_t\bar{w}_L\dot{\bar{w}}_L + 2C_{m_t}\left(\dot{\bar{w}}_L - L\dot{\Psi}_L\right) + 2\int_0^L \left(\rho A\bar{w}\dot{\bar{w}} + \rho I\psi\dot{\psi} - \vartheta\bar{w}'\dot{\bar{w}}'\right) dx \equiv \dot{I}_{tot} \quad (21)$$

$$\mu \triangleq \int_0^L (\rho A x\ddot{\bar{w}} + \rho I\ddot{\psi}) dx + I_h\ddot{\psi}_0 + m_t L\ddot{\bar{w}}_L + I_{m_t}\ddot{\psi}_L + C_{m_t}\left(\ddot{\Psi}\bar{w}_L - \ddot{\bar{w}}_L\Psi_L\right) \quad (22)$$

$$\vartheta \triangleq m_t L + \frac{1}{2}\rho A(L^2 - x^2) \quad (23)$$

3.1 Rayleigh-Ritz Approach

The uncoupling and solution of equations (14)-(16) is in general not possible, or under some assumptions is, at best, complicated. To this end, we seek an approximate solution via the Rayleigh-Ritz method.

As with all application of the Rayleigh-Ritz method, we introduce the trial functions for $\bar{w}$ and ψ such that

$$\bar{w}(x,t) \triangleq W^T(x)p(t) \quad \text{and} \quad \psi(x,t) \triangleq \Psi^T(x)q(t) \quad (24)$$

where $W(x)$ and $\Psi(x)$ are column matrices of basis functions and $p(t)$ and $q(t)$ are the vectors of undetermined parameters. These are defined as

$$W^T(x) = [W_1, W_2, \ldots, W_n] \qquad p(t) = [p_1, p_2, \ldots, p_n]^T \quad (25)$$

$$\psi^T(x) = [\Psi_1, \Psi_2, \ldots, \Psi_n] \qquad q(t) = [q_1, q_2, \ldots, q_n]^T \quad (26)$$

Oguamanam and Heppler [14] present a detailed discussion of the choice of the basis functions.

To obtain the equations of motion, we substitute (24) and their relevant derivatives into (7), (8), and (13). The resulting expressions are then used in the extended Hamilton's Principle (variations over $p, q,$ and θ) to obtain, after some manipulation,

$$\begin{bmatrix} \mu & M_{xW}^T + m_t L W_L^T & M_\Psi^T + I_h\Psi_0^T + I_{m_t}\Psi_L^T \\ M_{xW} + m_t L W_L & M_{WW} + m_t W_L W_L^T & 0 \\ M_\Psi + I_h\Psi_0 + I_{m_t}\Psi_L & 0 & M_{\Psi\Psi} + I_h\Psi_0\Psi_0^T + I_{m_t}\Psi_L\Psi_L^T \end{bmatrix} \begin{bmatrix} \ddot{\theta} \\ \ddot{p} \\ \ddot{q} \end{bmatrix} -$$

$$\dot{\theta}^2 \begin{bmatrix} 0 & 0 & 0 \\ 0 & M_{WW} + m_t W_L W_L^T - K_{\vartheta W'W'} & 0 \\ 0 & 0 & M_{\Psi\Psi} + I_{m_t} \Psi_L \Psi_L^T \end{bmatrix} \begin{bmatrix} \theta \\ p \\ q \end{bmatrix} +$$

$$\dot{\theta} C_{m_t} \begin{bmatrix} 0 & 2W_L^T & -2L\Psi_L^T \\ -\frac{1}{2}2W_L & 0 & -2W_L\Psi_L^T \\ \frac{1}{2}2L\Psi_L & 2W_L\Psi_L & 0 \end{bmatrix} \begin{bmatrix} \dot{\theta} \\ \dot{p} \\ \dot{q} \end{bmatrix} +$$

$$\ddot{\theta} C_{m_t} \begin{bmatrix} 0 & 2W_L^T & -2L\Psi_L^T \\ 0 & 0 & -\frac{1}{2}2W_L\Psi_L^T \\ 0 & \frac{1}{2}2W_L\Psi_L & 0 \end{bmatrix} \begin{bmatrix} \theta \\ p \\ q \end{bmatrix} +$$

$$C_{m_t} \begin{bmatrix} \begin{bmatrix} \ddot{p}^T & \ddot{q}^T \end{bmatrix} \begin{bmatrix} 0 & -W_L\Psi_L^T \\ W_L\Psi_L & 0 \end{bmatrix} \begin{bmatrix} p \\ q \end{bmatrix} \\ 0 \\ 0 \end{bmatrix} +$$

$$\ddot{\theta} \begin{bmatrix} \begin{bmatrix} p^T & q^T \end{bmatrix} \begin{bmatrix} M_{WW} + m_t W_L W_L^T - K_{\vartheta W'W'} & 0 \\ 0 & M_{\Psi\Psi} + I_{m_t} \Psi_L \Psi_L^T \end{bmatrix} \begin{bmatrix} p \\ q \end{bmatrix} \\ 0 \\ 0 \end{bmatrix} +$$

$$2\dot{\theta} \begin{bmatrix} \begin{bmatrix} \dot{p}^T & \dot{q}^T \end{bmatrix} \begin{bmatrix} M_{WW} + m_t W_L W_L^T - K_{\vartheta W'W'} & 0 \\ 0 & M_{\Psi\Psi} + I_{m_t} \Psi_L \Psi_L^T \end{bmatrix} \begin{bmatrix} p \\ q \end{bmatrix} \\ 0 \\ 0 \end{bmatrix} +$$

$$\begin{bmatrix} 0 & 0 & 0 \\ 0 & K_{W'W'} & -K_{W'\Psi} \\ 0 & -K_{W'\Psi}^T & K_{\Psi\Psi} + K_{B\Psi'\Psi'} \end{bmatrix} \begin{bmatrix} \theta \\ p \\ q \end{bmatrix} = \begin{bmatrix} M \\ 0 \\ M\Psi_0 \end{bmatrix} \tag{27}$$

with

$$\left.\begin{array}{ll} M_{WW} \triangleq \int_0^L \rho A W W^T dx, & M_{\Psi\Psi} \triangleq \int_0^L \rho I \Psi \Psi^T dx \\ M_{xW} \triangleq \int_0^L \rho A x W dx, & M_{\Psi} \triangleq \int_0^L \rho I \Psi dx \\ K_{W'W'} \triangleq \int_0^L \kappa G A W' W'^T dx, & K_{\Psi\Psi} \triangleq \int_0^L \kappa G A \Psi \Psi^T dx \\ K_{\vartheta W'W'} \triangleq \int_0^L \vartheta W' W'^T dx, & K_{B\Psi'\Psi'} \triangleq \int_0^L E I \Psi' \Psi'^T dx \\ K_{W'\Psi} \triangleq \int_0^L \kappa G A W' \Psi^T dx, & \mu \triangleq \frac{\rho A L^3}{3} + \rho I L + I_h + I_{m_t} + m_t L^2 \end{array}\right\} \tag{28}$$

For the purpose of this study, we have ignored the contributions of the first moment of the tip mass C_{m_t} since it's effect is negligible when compared with the effect of the second moment [2]. Further, we ignore the quadratic terms in p and q (i.e. $p^T(\ldots)p, q^T(\ldots)q, \dot{p}^T(\ldots)p$, and $\dot{q}^T(\ldots)q$), retaining only the nonlinear terms in θ. Making these simplifications yields

$$\begin{bmatrix} \mu & M_{xW}^T + m_t L W_L^T & M_{\Psi}^T + I_h \Psi_0^T + I_{m_t} \Psi_L^T \\ M_{xW} + m_t L W_L & M_{WW} + m_t W_L W_L^T & 0 \\ M_{\Psi} + I_h \Psi_0 + I_{m_t} \Psi_L & 0 & M_{\Psi\Psi} + I_h \Psi_0 \Psi_0^T + I_{m_t} \Psi_L \Psi_L^T \end{bmatrix} \begin{bmatrix} \ddot{\theta} \\ \ddot{p} \\ \ddot{q} \end{bmatrix} -$$

$$\dot{\theta}^2 \begin{bmatrix} 0 & 0 & 0 \\ 0 & M_{WW} + m_t W_L W_L^T - K_{\theta W' W'} & 0 \\ 0 & 0 & M_{\Psi\Psi} + I_{m_t} \Psi_L \Psi_L^T \end{bmatrix} \begin{bmatrix} \theta \\ p \\ q \end{bmatrix} + \begin{bmatrix} 0 & 0 & 0 \\ 0 & K_{W'W'} & -K_{W'\Psi} \\ 0 & -K_{W'\Psi}^T & K_{\Psi\Psi} + K_{B\Psi'\Psi'} \end{bmatrix} \begin{bmatrix} \theta \\ p \\ q \end{bmatrix} = \begin{bmatrix} M \\ 0 \\ M\Psi_0 \end{bmatrix} \quad (29)$$

Equation (27) is derived on the premise that a torque profile is specified. The equations of motion however take a different form when the velocity profile is specified. The equations of motion for a prescribed velocity profile are derived by taking the variations over p and q but not θ. After going through the manipulations, we arrive at the following equations of motion for the case of a prescribed velocity profile written in a matrix notation:

$$\begin{bmatrix} M_{WW} + m_t W_L W_L^T & 0 \\ 0 & M_{\Psi\Psi} + I_h \Psi_0 \Psi_0^T + I_{m_t} \Psi_L \Psi_L^T \end{bmatrix} \begin{bmatrix} \ddot{p} \\ \ddot{q} \end{bmatrix} + \begin{bmatrix} K_{W'W'} - \\ \dot{\theta}^2 \left(M_{WW} + m_t W_L W_L^T - K_{\theta W' W'} \right) & -K_{W'\Psi} \\ -K_{W'\Psi}^T & K_{\Psi\Psi} + K_{B\Psi'\Psi'} - \\ & \dot{\theta}^2 \left(M_{\Psi\Psi} + I_{m_t} \Psi_L \Psi_L^T \right) \end{bmatrix} \begin{bmatrix} p \\ q \end{bmatrix} = -\ddot{\theta} \begin{bmatrix} M_{xW} + m_t L W_L \\ M_\Psi + I_h \Psi_0 + I_{m_t} \Psi_L \end{bmatrix} \quad (30)$$

It is readily observed that for a constant velocity profile, the equations of motion correspond to an undamped, freely vibrating system.

4 Numerical Examples

The system is simulated, using two terms in the trial functions, for both a prescribed torque profile and a prescribed hub velocity profile. The hub velocity profile is chosen such that the root of the beam completes a rotation through an arc of θ_f radians in time t_*. This velocity profile is given as

$$\dot{\theta} = \begin{cases} 30 \frac{t^2}{t_*^3} \left[1 - \frac{t}{t_*} \left(2 - \frac{t}{t_*} \right) \right] \theta_f & t <= t_* \\ 0 & \text{otherwise} \end{cases} \quad (31)$$

and is illustrated in Figure 2.

In defining the torque profile, we choose the profile that will drive the beam through angle θ_f in time t_* assuming rigid-body motion. Thus

$$\mathcal{M} = \mu \ddot{\theta}$$

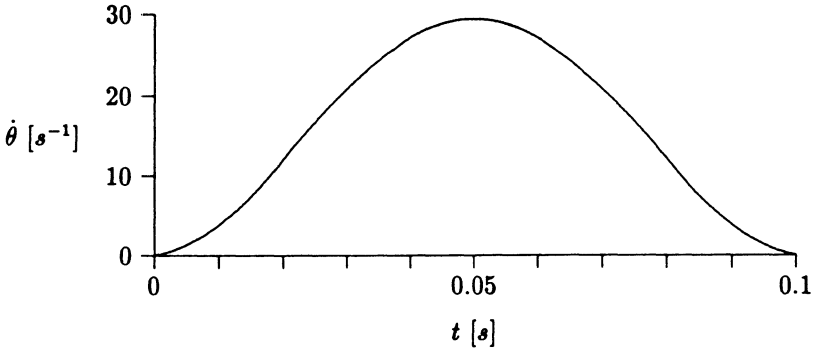

Figure 2: The prescribed hub velocity profile.

where μ is the total moment of inertia about the hub. The acceleration is obtained by differentiating (31) and is shown in Fig. 3.

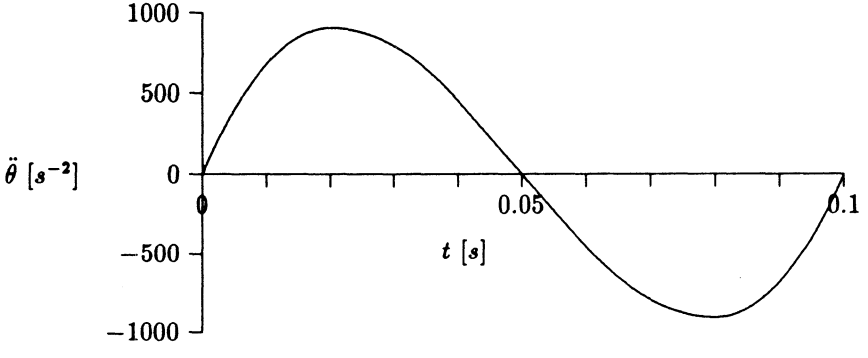

Figure 3: The prescribed hub acceleration ($\propto \mathcal{M}$) profile.

The material properties of the beam used in the examples are given in Table 1. The reported results are obtained for $t_* = 0.10$ s and $\theta_f = \frac{\pi}{2}$. The maximum velocity $\dot{\theta}$ attained in the prescribed hub velocity case was $\dot{\theta}_{max} = 29.45$ s^{-1} while the average velocity, evaluated over t_*, was $\dot{\theta}_{avg} = 15.71$ s^{-1}.

Figures 4 and 5 show the hub velocity and the tip displacement obtained using a prescribed torque profile for both the linear and the nonlinear systems with the beam height to length ratio of 0.005. In both plots the linear system is observed to exhibit higher vibration amplitude and lower frequency than the nonlinear system. These differences are attributable to the geometric stiffening effect. Because centrifugal forces are not ignored in the nonlinear system, the beam reacts to these tensile forces by stiffening.

Parameter	Value
L	0.725 m
E	6.5×10^{10} Pa
G	2.8×10^{10} Pa
ρ	2.753×10^{3} Pa
A	3.175×10^{4} m^2
h	0.0725 m and 0.03625 m
I_h	1.25×10^{-3} kgm^2
m_t	ρAL
I_{m_t}	1.25×10^{-3} kgm^2

Table 1: Beam Material Properties.

The effect is that the amplitude of the flexural vibration of the beam is reduced while the frequency is increased when compared to the corresponding linear system.

The corresponding plot of tip displacement for a prescribed velocity

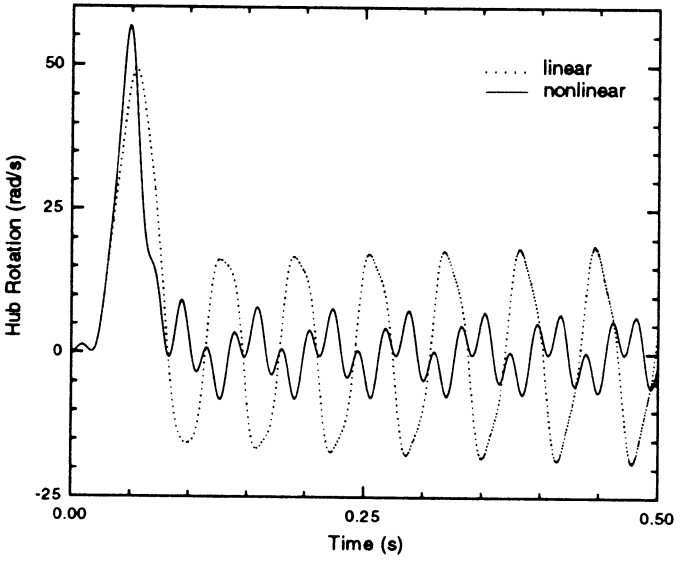

Figure 4: Hub velocity; $h/L = 0.005$, prescribed torque profile.

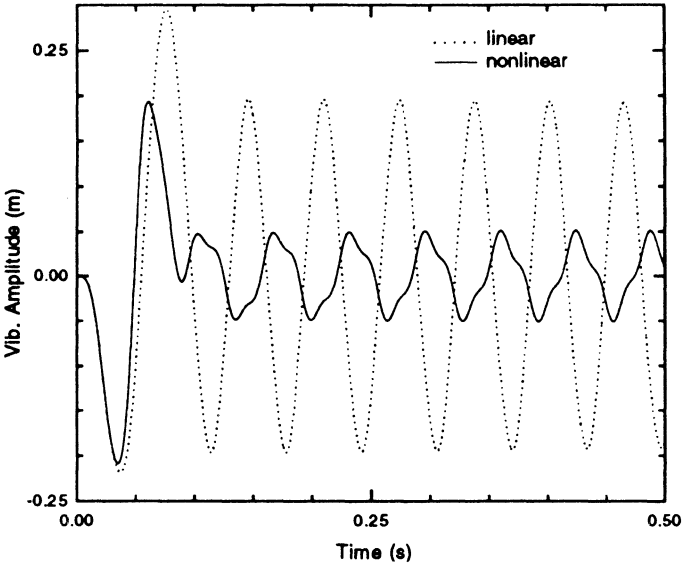

Figure 5: Tip displacement; $h/L = 0.005$, prescribed torque profile.

profile is given in Fig. 6. As observed earlier with the torque profile, the vibration amplitude and frequency of the linear system are respectively higher and lower than those observed in the nonlinear system. Again, this is due to the geometric stiffening.

It is worth mentioning that the difference in the amplitudes of the responses for the prescribed torque profile and the prescribed velocity profile is because the derivation of the two systems is intrinsically different. For example, while the hub velocity at the end of t_* is zero for the case of a prescribed velocity profile, it fluctuates about zero in the prescribed torque profile scenario. Elastic motion was ignored in defining the torque profile thus the resulting hub velocity profile obtained at the end of the simulation is actually superimposed with the elastic velocity.

The hub velocity and the tip displacement for a prescribed torque profile for both linear and nonlinear systems with beam height to length ratio of 0.01 is depicted in Figs. 7 and 8. The observations made previously for the thinner beam ($h/L = 0.005$) are valid here but only for the first 0.10 *secs*, which is the duration of the applied torque. The question is

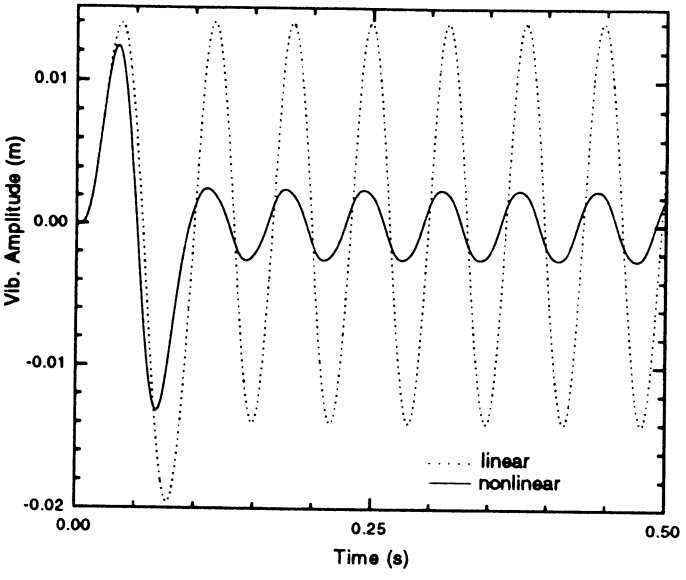

Figure 6: Tip displacement; $h/L = 0.005$, prescribed velocity profile.

why the reversal in amplitude when the torque is removed. Clearly the slenderness of the beam is the contributing factor in these results with the less slender beam not experiencing any significant difference between the linear and the nonlinear cases for this input torque.

The observations made of the response curve for the prescribed torque profile for the case where the beam height to length ratio is 0.01 are again tenable in the case of a prescribed velocity profile, see Fig. 9.

5 Summary

We have discussed the influence of geometric stiffening on a beam that is attached to a rotating base. The equations of motion are derived using the extended Hamilton's Principle and the Rayleigh-Ritz method was used to obtain an approximate solution. The results from the numerical study indicate that modelling the beam without the inclusion of geometric stiffening effects would lead to a system that underestimates the flexural amplitude and overestimates the frequency. These are in agreement with our engineer-

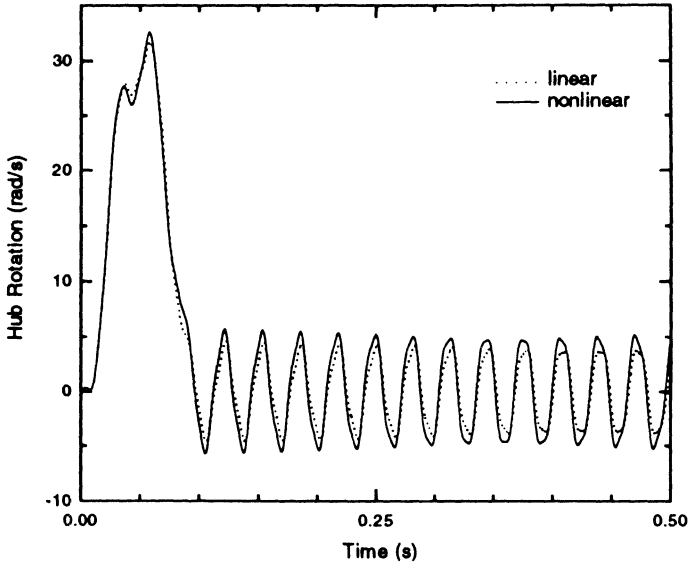

Figure 7: Hub velocity; $h/L = 0.01$, prescribed torque profile.

ing intuition. However, depending on the flexibility of the beam, the same system is observed to overestimate the flexural amplitude and underestimate the frequency when the applied torque is removed. We attribute this result to a transverse component of the centrifugal force. The interaction between the tip mass, beam mass and flexibility is complex and one that requires further understanding. We have presented our results using the first two modes, but it would be preferable to use more terms in the trial functions to better capture the dynamics of the nonlinear system.

References

[1] Haung, T.S., "The Effect of Rotatory Inertia and of Shear Deformation on the Frequency and Normal Mode Equations of Uniform Beams with Simple End Conditions", *J. Appl. Mech.*, **28**, 1961, 579-584.

[2] White, M.W.D., and Heppler, G.R., "Vibration Modes and Frequencies of Timoshenko Beams with Attached Rigid Bodies", *ASME J. Appl. Mech.*, **62**, 1995, 193-199.

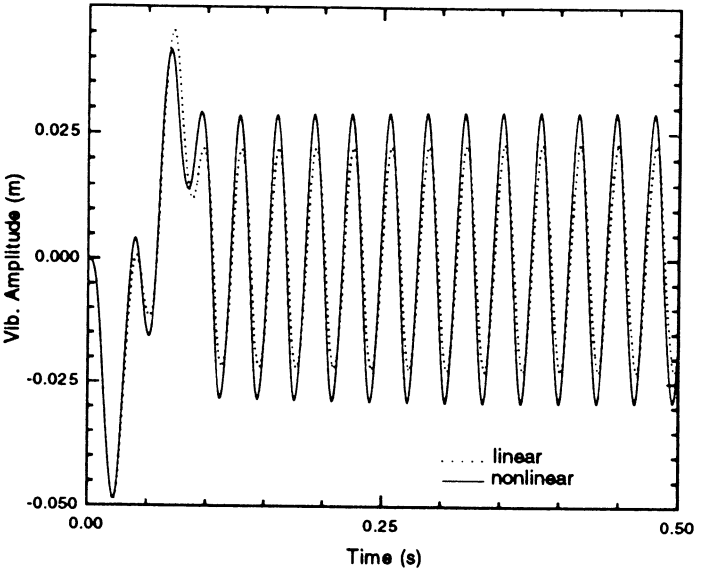

Figure 8: Tip displacement; $h/L = 0.01$, prescribed torque profile.

[3] Mitchell, T. P., and Bruch, J. C., "Free Vibration of a Flexible Arm Attached to a Complaint Finite Hub", *J. of Vibration, Acoustics, Stress, and Reliability in Design*, **110**, 1988, 118-120.

[4] Bellezza, F., Lanari, L., and Ulivi, G., "Exact Modeling of the Flexible Slewing Link", *Proc. IEEE Int. Conf. on Rob. and Auto.*, Cincinatti, Ohio, **3**, 1990, 734-739.

[5] White, M. W. D., Heppler, G. R., "A Timoshenko Model of A Flexible Slewing Link" Proc. 1995 American Control Conference, Seattle WA, June 21-23, 1995. 4 2815-2819.

[6] Kojima, H., "Transient Vibrations of a Beam/Mass System Fixed to a Rotating Body", *J. of Sound and Vibration*, **107**, no. 1, 1986, 149-154.

[7] Yigit, A., Scott, R.A., and Ulsoy, A.G., "Flexural Motion of a Radially Rotating Beam Attached to a Rigid Body", *J. of Sound and Vibration*, **121**, no. 2, 1988, 201-210.

[8] Damaren, C., and Sharf, I., "Simulation of Flexible-Link Manipulators with Inertia and Geometric Nonlinearities", *J. of Dynamic Systems, Measurement and Control*, **117**, 1995, 74-87.

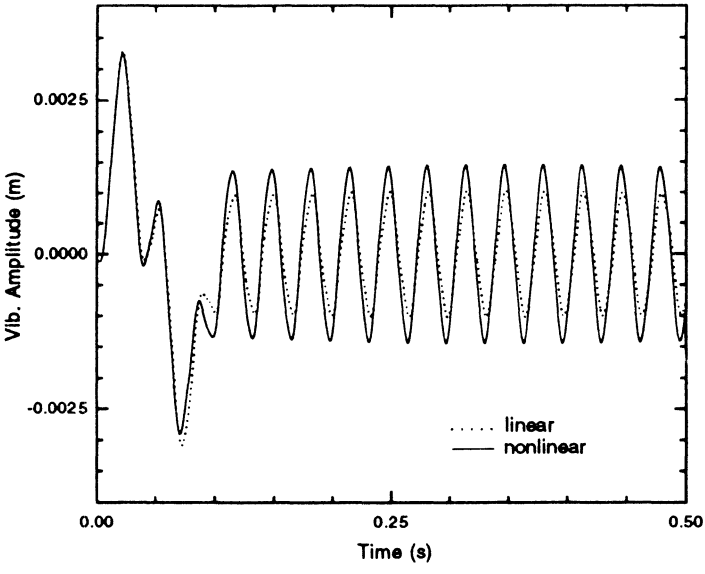

Figure 9: Tip displacement; $h/L = 0.01$, prescribed velocity profile.

[9] M.J. Sadigh, A.K. Misra, "More on the So-Called Dynamic Stiffening Effect", *J. Astro. Sci.*, **43**, No. 2, 1995, 101-125.

[10] I. Sharf, "Geometric Stiffening in Multibody Dynamics Formulations", *AIAA J. Guid. Cont. & Dyn.*, **18**, No. 4, 882-890.

[11] S. Timoshenko, D. H. Young, W. Weaver, Jr., Vibration Problems in Engineering, Fourth Ed., John Wiley & Sons, New York, 1974.

[12] F.Y. Wang, G. Guan, "Influences of Rotating Inertia, Shear, and Loading on Vibrations of Flexible Manipulators", *J. Sound and Vibration*, **171**, 1994, 433-452.

[13] Peter C. Hughes, *Spacecraft Attitude Dynamics*, John Wiley & Sons, New York, 1986.

[14] D.C.D. Oguamanam, G.R. Heppler, *Centrifugal Stiffening of a Timoshenko Beam*, ConStruct Technical Report, TR95-001, University of Waterloo, 1995.